

A NEW SET OF ASYMMETRIC FILTERS FOR TRACKING THE SHORT-TERM TREND IN REAL-TIME

BY ESTELA BEE DAGUM AND SILVIA BIANCONCINI

University of Bologna

For assessing in real time the short-term trend of major economic indicators, official statistical agencies generally rely on asymmetric filters that were developed by Musgrave in 1964. However, the use of the latter introduces revisions as new observations are added to the series and, from a policy-making viewpoint, they are too slow in detecting true turning points. In this paper, we use a reproducing kernel methodology to derive asymmetric filters that converge quickly and monotonically to the corresponding symmetric one. We show theoretically that proposed criteria for time-varying bandwidth selection produce real-time trend-cycle filters to be preferred to the Musgrave filters from the viewpoint of revisions and time delay to detect true turning points. We use a set of leading, coincident and lagging indicators of the US economy to illustrate the potential gains statistical agencies could have by also using our methods in their practice.

1. Introduction. In recent years, statistical agencies have shown an interest in providing trend-cycle or smoothed seasonally adjusted graphs to evaluate the stage of the cycle at which the economy stands. This is known as recession and recovery analysis, and differs from business cycle studies where cyclical fluctuations are measured around a long-term trend to estimate complete business cycles [see, e.g., Azevedo (2011), Azevedo, Koopman and Rua (2006), Christiano and Fitzgerald (2003), de Carvalho, Rodrigues and Rua (2012), de Carvalho and Rua (2014), Hodrick and Prescott (1997)]. Among other reasons, this interest originated from the recent crisis and major economic and financial changes of global nature which have introduced more variability in the data. The US entered in recession in December 2007 till June 2009, and this has produced a chain reaction all over the world. There is no evidence of a fast recovery as in previous recessions. The economic growth is sluggish and high levels of unemployment have been observed. It has become difficult to determine the direction of the short-term trend by simply looking at month to month (quarter to quarter) changes of seasonally adjusted values, particularly to assess the upcoming of a true turning point. Failure in providing reliable trend-cycle estimates in real time could lead to the adoption of counteract policies that will affect the whole economy in a negative way.

Received September 2014; revised June 2015.

Key words and phrases. Recession and recovery analysis, reproducing kernels, seasonally adjusted data, Musgrave filters, time-varying bandwidth selection, US economy.

The linear filter developed by Henderson (1916) is one of the most frequently applied to estimate the trend-cycle component of seasonally adjusted economic indicators. It is available in nonparametric seasonal adjustment software, such as the US Bureau of the Census X11 method [Shiskin, Young and Musgrave (1967)] and its variants, X11/X12ARIMA and X13. The Henderson smoother has the property that fitted to exact cubic functions will reproduce their values, and fitted to stochastic cubic polynomials it will give smoother results than those estimated by ordinary least squares. The properties and limitations of the Henderson filters have been extensively discussed by many authors, among them, Cholette (1981), Kenny and Durbin (1982), Dagum and Laniel (1987), Dagum (1996), Gray and Thomson (1996), Loader (1999), Ladiray and Quenneville (2001), Findley and Martin (2006), Dagum and Luati (2009a, 2012). Dagum and Bianconcini (2008) represented the Henderson filter using Reproducing Kernel Hilbert Space (RKHS) methodology [we refer the reader to Berlinet and Thomas-Agnan (2004) for a detail description of RKHS]. Their approach is based on a theoretical result due to Berlinet (1993), according to which a kernel estimator of order p can always be decomposed into the product of a reproducing kernel R_{p-1} , belonging to the space of polynomials of degree at most $p - 1$, and a probability density function f_0 with finite moments up to order $2p$. The authors found that a kernel function obtained as the product of the biweight density function and the sum of its orthonormal polynomials is particularly suitable when the length of the filter is rather short, say, between 5 to 23 terms, which are those often applied by statistical agencies.

At the beginning and end of the sample period, the Henderson filter of length, say, $2m + 1$, cannot be applied to the m data points, hence, only asymmetric filters can be used. The estimates of the real time trend are then subject to revisions due to the innovations brought by the new data entering in the estimation and to the fact that the asymmetric filters are time varying in the sense of being different for each of the m data points.

In this paper, we propose a new set of asymmetric weights to replace the Musgrave ones officially adopted by statistical agencies to detect the direction of the short-term trend in real time. From an applied viewpoint, we are motivated by the need of obtaining reliable short-term estimates in real time, which can be more useful from a policy-making viewpoint. We apply the new filters to leading, coincident and lagging indicators of the US economy, which is known to be a key player from an international macroeconomic perspective. We will concentrate on the reduction of revisions only due to filter changes, and ignore those introduced by new innovations entered with new data. In other words, the filter revisions depend on how close the asymmetric filters are with respect to the symmetric one [Dagum (1996), Dagum and Laniel (1987)]. Besides the filter revisions, we shall deal with the time delay to identify the upcoming of a true turning point. Another important property analyzed for the new set of asymmetric filters is the time path followed by the last trend-cycle point as new observations are added to the series. This is obtained by calculating the number of months (quarters) it takes for the

last trend-cycle estimate to identify a true turning point in the same position of the final trend-cycle data. An optimal asymmetric filter should have a time path that converges fast and monotonically to the final estimate as new observations are added to the series.

Several authors have studied the properties and limitations of the Musgrave filters [Doherty (2001), Gray and Thomson (2002), Laniel (1985), Quenneville, Ladiray and Lefrancois (2003), Dagum and Luati (2009b, 2012), Bianconcini and Quenneville (2010)]. Dagum and Bianconcini (2008, 2013) introduced a RKHS representation of the asymmetric filters of Musgrave (1964). In the RKHS framework, given the density function (in our case the biweight), once the length of the symmetric filter is chosen, say $2m + 1$, the statistical properties of the asymmetric filters are strongly affected by the bandwidth parameter of the kernel function from which the weights are derived. In previous works, Dagum and Bianconcini (2008, 2013) made the bandwidth parameters equal for all the asymmetric filters (global time-invariant bandwidth) to closely approximate the Musgrave filters.

Additionally, we propose here time varying bandwidth parameters since the asymmetric filters are time varying. We consider three specific criteria of bandwidth selection based on the minimization of the following:

1. the distance between the transfer functions of asymmetric and symmetric filters,
2. the distance between the gain functions of asymmetric and symmetric filters, and
3. the phase shift function over the domain of the signal.

Section 2 presents a motivating example using the US New Orders for Durable Goods (NODG) series. Section 3 gives the RKHS representations of the Henderson and Musgrave linear filters, and discusses the discretization of the continuous kernel functions when applied to data. Section 4 deals with the time-varying optimal bandwidth selection where a filter is defined as optimal if: (1) it minimizes the revisions between last point and final trend-cycle values as new observations are added, and (2) reduces the time delay to signal the upcoming of a true turning point. Section 5 provides an empirical application to leading, coincident and lagging indicators of the US economy. Finally, Section 6 gives the conclusions.

2. Motivating example: US new orders for durable goods. The monthly series of US New Orders for Durable Goods (NODG), published by the US Census Bureau, measures the volume of orders of goods whose intended lifespan is three years or more. Approximately 60 percent of the orders are for cars and trucks, with building materials, furniture and household items accounting for most of the remaining part. The NODG series is a leading indicator of US manufacturing activity, and an increase in orders is considered as more future business for manufacturers. The market often moves on accordingly in spite of its high volatility, hence, it represents an important indicator of the state of the economy, allowing to detect

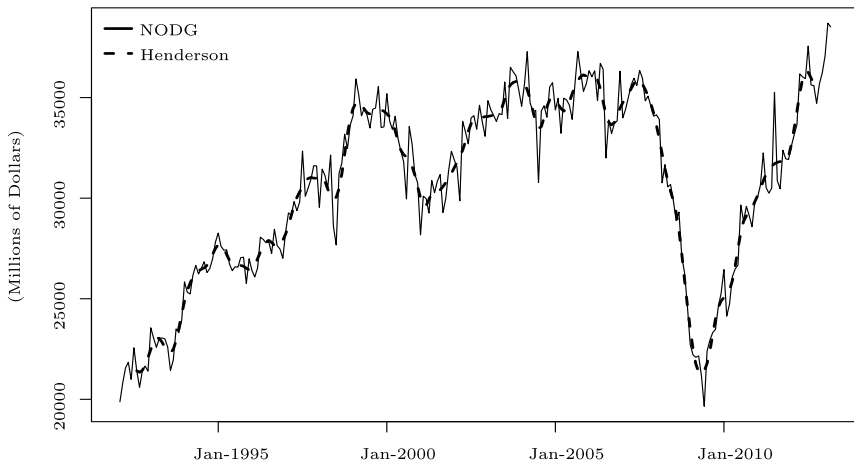


FIG. 1. *New Orders for Durable Goods, US: seasonally adjusted series and trend-cycle estimates obtained with the 13-term Henderson filter. Source: US Census Bureau.*

shifts in the US economy up to six months in advance. Figure 1 illustrates the final vintage data of the monthly NODG series for the period February 1992–March 2013. It is evident that the NODG peaked in the middle of 2007, and underwent thenceforth a very steep decline up to June 2009, that has been identified by the Business Cycle Dating Committee of the National Bureau of Economic Research (NBER) to be the last trough in the US economy. The dashed line overlaid to the seasonally adjusted NODG series in Figure 1 is the nonparametric estimate of the corresponding trend-cycle component produced by the application of the 13-term symmetric filter due to Henderson (1916).

It is evident from Figure 1 that the two-sided estimates of the signal are not available for the first and last six months, the latter being the most important for short-term trend prediction. The corresponding estimates are derived using asymmetric filters due to Musgrave (1964). They are known to possess the good property of fast detection of turning points, but they tend to introduce large revisions when new observations are added to the series. This is illustrated in Figure 2 for the last point Musgrave filter that is the most important since it provides the real time trend-cycle estimate corresponding to the current observation. Besides the phase shift effect typical of asymmetric filters, that produces a temporal displacement of the point of maxima and minima of the input series, a crude measure of the size of the total revision of the asymmetric filter is given by the distance, for each point in time, between the estimate obtained by its application (long dash line) and the final estimate derived by using the symmetric filter (solid line).

To overcome the main limitations of the Musgrave filters, Dagum and Bianconcini (2008) have provided an equivalent kernel representation of the symmetric Henderson filter and derived the corresponding asymmetric filters using the Reproducing Kernel Hilbert Space (RKHS) methodology. The main advantage of

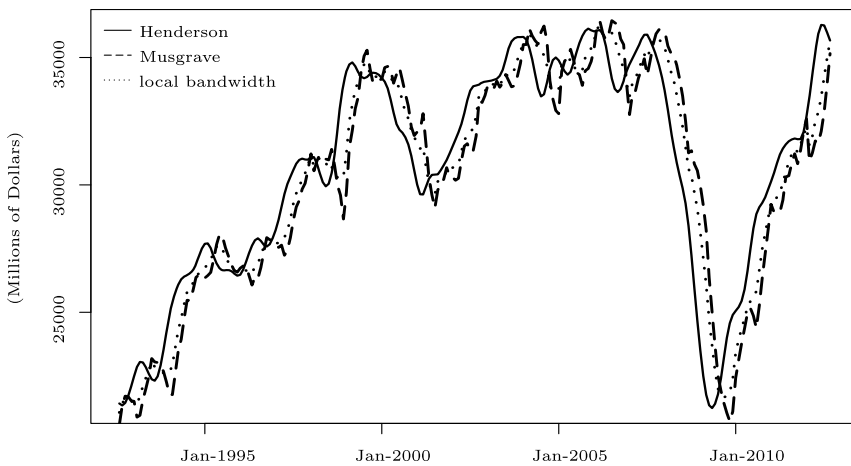


FIG. 2. *New Orders for Durable Goods, US: trend-cycle estimates based on Henderson filter, last point Musgrave and RKHS asymmetric filters, respectively.*

the asymmetric kernel filters with respect to the Musgrave ones is that the former are derived following the same criteria as the symmetric filter, whereas the latter are determined based on different optimization criteria. Having chosen the length of the filter, the properties of these asymmetric kernels are strongly dependent on bandwidth parameters. The current authors originally made the bandwidth parameter equal for all the asymmetric filters (global time-invariant bandwidth) to closely approximate the Musgrave filters and ensure a fast convergence to the corresponding symmetric one.

In this paper, several criteria for bandwidth selection are proposed based on specific properties that the corresponding asymmetric filters should satisfy. As a specific case, Figure 2 shows the behavior of the last point kernel filter whose bandwidth parameter has been selected in order to ensure more accurate predictions. In particular, the latter has been chosen to minimize the distance between the gain functions of the last point and symmetric kernel filters. It can be noticed that over the whole sample span, the kernel filter (dotted line) is the closest to the final estimates (solid line). As discussed in the subsequent sections, the revisions are almost 50 percent smaller than those introduced by the Musgrave filter. However, it should be noticed that a reduction in the revisions does not necessarily imply a reduction in the time lag to signal the upcoming of a true turning point. This is obtained by calculating the number of months it takes for the revised real time trend-cycle to signal a turning point in the same position as in the final trend-cycle series. For the June 2009 turning point observed for the NODG series, this is illustrated in Figure 3 for the last point Musgrave (right) and optimal kernel (left) filters. This figure gives the revision path of the last available point (June 2009) as we keep adding one observation at a time up to December 2009, when the final estimate is achieved. It can be noticed that after adding only one month to the series

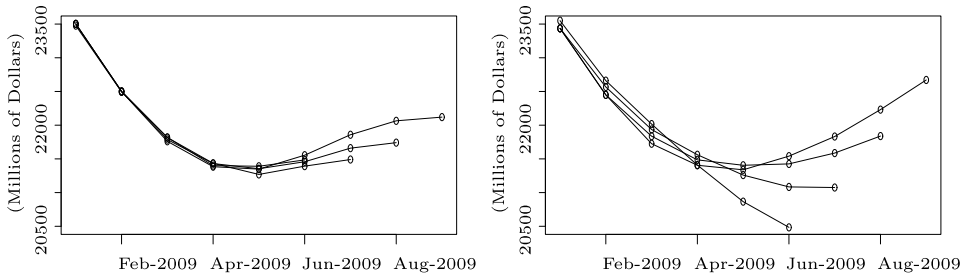


FIG. 3. US NODG series. Revision path of the June 2009 (turning point) estimate as one observation is added at a time up to December 2009 (final estimate) using the optimal last point asymmetric kernel (left) and Musgrave (right) filters, respectively.

ending in June, the turning point is clearly detected by the RKHS filter, whereas two months are required by the Musgrave filter.

Full details will be given in the sequel; it suffices to say at this point that the set of asymmetric filters for detecting the short-term trend in real time introduced in this study provides better estimates than the classically applied Musgrave filters. The improvements are reflected in the size of total revisions and time delay to identify the upcoming of a true turning point. This is illustrated more extensively in Section 5.

3. Linear filters in RKHS. Let $\{y_t, t = 1, \dots, N\}$ denote the input series, supposed to be seasonally adjusted where trading day variations and extreme values, if present, have been also removed. We assume that it can be decomposed into the sum of a systematic component (signal) g_t , that represents the trend and cycle usually estimated jointly, plus an erratic component u_t , called the noise, such that

$$(3.1) \quad y_t = g_t + u_t.$$

The noise u_t can be either a white noise, $WN(0, \sigma_u^2)$, or, more generally, a stationary and invertible AutoRegressive Moving Average (ARMA) process. On the other hand, the signal $g_t, t = 1, \dots, T$, is assumed to be a smooth function of time, such that it can be represented *locally* by a polynomial of degree p in a variable j , which measures the distance between y_t and its neighboring observations $y_{t+j}, j = -m, \dots, m$. This is equivalent to estimating the trend-cycle \hat{g}_t as a weighted moving average as follows:

$$(3.2) \quad \hat{g}_t = \sum_{j=-m}^m w_j y_{t+j} = \mathbf{w}'\mathbf{y}, \quad t = m + 1, \dots, N - m,$$

where $\mathbf{w}' = [w_{-m} \dots w_0 \dots w_m]$ contains the weights to be applied to the input data $\mathbf{y}' = [y_{t-m} \dots y_t \dots y_{t+m}]$ to get the estimate \hat{g}_t for each point in time.

Several nonparametric estimators, based on different sets of weights \mathbf{w} , have been developed in the literature. The Henderson filter [Henderson (1916), Kenny

and Durbin (1982), Ladiray and Quenneville (2001), Loader (1999)] results from fitting a cubic polynomial to the input values \mathbf{y} by means of weighted least squares, that is,

$$(3.3) \quad \min_{\boldsymbol{\beta}} [\mathbf{y} - \mathbf{X}\boldsymbol{\beta}]' \mathbf{W} [\mathbf{y} - \mathbf{X}\boldsymbol{\beta}],$$

where

$$\mathbf{X} = \begin{bmatrix} 1 & -m & m^2 & -m^3 \\ 1 & -(m-1) & (m-1)^2 & -(m-1)^3 \\ \vdots & \cdots & \cdots & \vdots \\ 1 & 0 & 0 & 0 \\ \vdots & \cdots & \cdots & \vdots \\ 1 & (m-1) & (m-1)^2 & (m-1)^3 \\ 1 & m & m^2 & m^3 \end{bmatrix}, \quad \boldsymbol{\beta} = \begin{bmatrix} \beta_0 \\ \beta_1 \\ \beta_2 \\ \beta_3 \end{bmatrix},$$

and $\mathbf{W} = \text{diag}(W_{-m}, \dots, W_0, \dots, W_m)$ with generic element $W_j \propto \{(m+1)^2 - j^2\}\{(m+2)^2 - j^2\}\{(m+3)^2 - j^2\}$, chosen as to minimize the sum of squares of the third differences of the weights \mathbf{w} . As discussed by Loader (1999), the latter are given by the product of a cubic polynomial $\phi(j)$ and W_j , such that

$$\hat{g}_t = \sum_{j=-m}^m \phi(j) W_j y_{t+j}.$$

For large m , Loader (1999) provided an equivalent kernel representation of the weights by showing that W_j can be approximated by the triweight function $m^6(1 - (j/m)^2)^3$, such that the weight diagram is approximately $(315/512)(3 - 11(j/m)^2)(1 - (j/m)^2)^3$.

Different kernel characterizations of the Henderson filter have been derived by Dagum and Bianconcini (2008, 2013) based on the Reproducing Kernel Hilbert Space (RKHS) methodology. A RKHS is a Hilbert space characterized by a kernel that reproduces, via an inner product, every function of the space. It follows that a kernel estimator of order p can always be decomposed into the product of a reproducing kernel R_{p-1} , belonging to the space of polynomials of degree at most $p-1$, and a probability density function f_0 with finite moments up to order $2p$ [Berliner (1993)]. In this context, the equivalent kernel representation of the Henderson filter is given by

$$(3.4) \quad K_4(t) = \sum_{i=0}^3 P_i(t) P_i(0) f_0(t), \quad t \in [-1, 1],$$

where f_0 is the density function, defined on $[-1, 1]$, obtained through normalization of W_j , and the P_i are the corresponding orthonormal polynomials. Equiva-

lently, the kernel in (3.4) can be written as

$$(3.5) \quad K_4(t) = \frac{\det(\mathbf{H}_4^0[1, \mathbf{t}])}{\det(\mathbf{H}_4^0)} f_0(t), \quad t \in [-1, 1],$$

where \mathbf{H}_4^0 is the Hankel matrix whose elements are the moments of f_0 , that is, $\mu_r = \int_{-1}^1 t^r f_0(t) dt$. In particular, the first row contains the moments from μ_0 to μ_3 , whereas the last row those from μ_3 to μ_6 . $\mathbf{H}_4^0[1, \mathbf{t}]$ is the matrix obtained by replacing the first column of \mathbf{H}_4^0 by the vector $\mathbf{t} = [1 \ t \ t^2 \ t^3]'$.

The density f_0 depends on W_j , hence, on the length of the filter, and it needs to be determined any time that m changes. The kernel representation based on the triweight function allows to overcome such limitation, but [Dagum and Bianconcini \(2008\)](#) have found that the biweight function $f_{0B}(t) = (15/16)(1 - t^2)^2, t \in [-1, 1]$, provides a better approximation for Henderson filters of short length, say, between 5 to 23 terms which are those used by statistical agencies [see also [Bianconcini and Quenneville \(2010\)](#)].

When applied to real data, the symmetric filter weights are derived as follows:

$$(3.6) \quad w_j = \frac{K_4(j/b)}{\sum_{j=-m}^m K_4(j/b)}, \quad j = -m, \dots, m,$$

where b is a time-invariant global bandwidth parameter (same for all $t = m + 1, \dots, N - m$) selected to ensure a symmetric filter of length $2m + 1$. The bandwidth parameter relates the discrete domain of the filter, that is, $\{-m, \dots, m\}$, with the continuous domain of the kernel function, that is, $[-1, 1]$. The weights given in (3.6) can be also rewritten in matrix form as follows.

PROPOSITION 3.1. *The weights \mathbf{w} derived using the kernel function in (3.4) admit the following representation:*

$$(3.7) \quad \mathbf{w}' = \mathbf{e}'_1 \mathbf{H}_s^{-1} \mathbf{X}'_b \mathbf{F}_b,$$

where $\mathbf{e}'_1 = [1 \ 0 \ 0 \ 0]$, $\mathbf{H}_s = \mathbf{H}_4^0[1, \mathbf{S}]$ with $\mathbf{S}' = [S_0 \ 0 \ S_2 \ 0]$, being $S_r = b^{-1} \sum_{j=-m}^m (j/b)^r f_0(j/b)$ the discrete approximation of μ_r , and b the bandwidth parameter. In addition, \mathbf{X}_b has the same form as \mathbf{X} in (3.3), but with generic row given by $[1 \ j/b \ (j/b)^2 \ (j/b)^3]$, $j = -m, \dots, m$, and $\mathbf{F}_b = \text{diag}(1/bf_{0B}(-m/b), \dots, 1/bf_{0B}(m/b))$.

A formal proof of Proposition 3.1 is provided in the [Appendix](#). It can be easily shown that the generic element of \mathbf{w} is given by

$$(3.8) \quad w_j = \left[\frac{\mu_4 - \mu_2(j/b)^2}{S_0\mu_4 - S_2\mu_2} \right] \frac{1}{b} f_{0B}\left(\frac{j}{b}\right), \quad j = -m, \dots, m.$$

In this setting, once the length of the filter is selected, the choice of the bandwidth parameter b is fundamental. It has to be chosen to ensure that only, say, $2m + 1$

observations surrounding the target point will receive nonzero weights as well as to approximate, as close as possible, the continuous density function with the discrete one as well as its moments. Indeed, we can separate (3.7) into two parts. One concerns the discretization of the density function f_0 in terms of adjacent rectangles, erected over discrete intervals, whose width is determined by the bandwidth b . The second part corresponds to the discretization of the reproducing kernel that depends on the discrete moments S_0 and S_2 . Of these two parts, the former plays the most important role to approximate the continuous kernel given in (3.4) for the Henderson filter representation. Its bandwidth parameter selection is done to guarantee specific inferential properties of the trend-cycle estimators. In this regard, [Dagum and Bianconcini \(2008, 2013\)](#) used a time-invariant global bandwidth b equal to $m + 1$, which gave excellent results.

3.1. Asymmetric filters. The derivation of the symmetric Henderson filter has assumed the availability of $2m + 1$ input values centered at t . However, at the end of the sample period, that is, $t = N - (m + 1), \dots, N$, only $2m, \dots, m + 1$ observations are available, and asymmetric filters of the same length have to be considered. Hence, at the boundary, the effective domain of the kernel function K_4 is $[-1, q^*]$, with $q^* \ll 1$, instead of $[-1, 1]$ as for any interior point. This implies that the symmetry of the kernel is lost, and it does not integrate to unity on the asymmetric support $[\int_{-1}^{q^*} K_4(t) dt \neq 1]$. Furthermore, the moment conditions are no longer satisfied, that is, $\int_{-1}^{q^*} t^i K_4(t) dt \neq 0$, for $i = 1, 2, 3$. To overcome these limitations, several boundary kernels have been proposed in the literature.

In the context of real time trend-cycle estimation, the condition that the kernel function integrates to unity is essential, whereas the unbiasedness property can only be satisfied with a great increase in the variance of the estimates. This is a consequence of the well-known trade-off between bias and variance. This latter becomes very large because most of the contribution to the real time trend-cycle estimates comes from the current observation which gets the largest weight. Based on these considerations, [Dagum and Bianconcini \(2008, 2013\)](#) have suggested following the so-called “cut and normalize” method [[Gasser and Müller \(1979\)](#), [Kyung-Joon and Schucany \(1998\)](#)], according to which the boundary kernels $K_4^{q^*}$ are obtained by cutting the symmetric kernel K_4 to omit that part of the function lying between q^* and 1, and by normalizing it on $[-1, q^*]$. That; that is,

$$(3.9) \quad K_4^{q^*}(t) = \frac{K_4(t)}{\int_{-1}^{q^*} K_4(t) dt} = \frac{\det(\mathbf{H}_4^0[1, \mathbf{t}]) f_{0B}(t)}{\det(\mathbf{H}_4^0[1, \boldsymbol{\mu}^{q^*}])}, \quad t \in [-1, q^*],$$

where $\boldsymbol{\mu}^{q^*} = [\mu_0^{q^*} \mu_1^{q^*} \mu_2^{q^*} \mu_3^{q^*}]$ with $\mu_r^{q^*} = \int_{-1}^{q^*} t^r f_{0B}(t) dt$ being proportional to the moments of the truncated biweight density f_{0B} on the support $[-1, q^*]$, which from now on we simply refer to as truncated moments.

Applied to real data, the “cut and normalize” method yields the following formula for the asymmetric weights:

$$(3.10) \quad w_{q,j} = \frac{K_4^{q*}(j/b_q)}{\sum_{j=-m}^q K_4^{q*}(j/b_q)} = \frac{\det(\mathbf{H}_4^0[1, \mathbf{j}/\mathbf{b}_q])(1/b_q) f_{0B}(j/b_q)}{\det(\mathbf{H}_a)}$$

for $j = -m, \dots, q$, and $q = 0, \dots, m - 1$, where $b_q, q = 0, \dots, m - 1$, is the local bandwidth, specific for each asymmetric filter. As before, b_q allows us to relate the discrete domain of the filter, that is, $\{-m, \dots, q\}$, for each $q = 0, \dots, m - 1$, to the continuous domain of the kernel function, that is, $[-1, q^*]$. Furthermore, $\mathbf{j}/\mathbf{b}_q = [1 (j/b_q) (j/b_q)^2 (j/b_q)^3]$, and $\mathbf{H}_a = \mathbf{H}_4^0[1, \mathbf{S}^q]$ with $\mathbf{S}^q = [S_0^q S_1^q S_2^q S_3^q]'$, and $S_r^q = \sum_{j=-m}^q (1/b_q)(j/b_q)^r f_{0B}(j/b_q)$ the discrete approximation of μ_r^{q*} .

PROPOSITION 3.2. *Each asymmetric filter $\mathbf{w}_q = [w_{q,-m} \dots w_{q,q}]'$ of length $(m + q + 1)$, for $q = 0, \dots, m - 1$, admits the following matrix representation:*

$$(3.11) \quad \mathbf{w}'_q = \mathbf{e}'_1 \mathbf{H}_a^{-1} \mathbf{X}'_q \mathbf{F}_q, \quad q = 0, \dots, m - 1,$$

where \mathbf{X}_q is a matrix of dimensions $(m + q + 1) \times 4$, whose generic row is given by $\mathbf{j}/\mathbf{b}_q, j = -m, \dots, q$, and $\mathbf{F}_q = \text{diag}((1/b_q) f_{0B}(-m/b_q), \dots, (1/b_q) f_{0B}(q/b_q))$. It can be easily shown that the generic element of \mathbf{w}_q is

$$(3.12) \quad w_{q,j} = \left[\frac{\mu_4 - \mu_2(j/b_q)^2}{S_0^q \mu_4 - S_2^q \mu_2} \right] \frac{1}{b_q} f_{0B}\left(\frac{j}{b_q}\right),$$

where $j = -m, \dots, q$ and $q = 0, \dots, m - 1$.

The proof of Proposition 3.2 is similar to that of Proposition 3.1 and, for space reasons, is omitted.

3.1.1. *Properties of the asymmetric filters.* Since the trend-cycle estimates for the last m data points do not use $2m + 1$ observations for any interior point, but $2m, 2m - 1, \dots, m + 1$ data, they are subject to revisions due to the following: (1) new observations entering in the estimation and (2) filter changes. As said before, we will concentrate on the reduction of revisions due to filter changes. The reduction of these revisions is an important property that the asymmetric filters should possess together with a fast detection of true turning points. In the specific case of the RKHS filters, (3.12) shows how the asymmetric filter weights are related to the symmetric ones given in (3.8). It is clear that the convergence depends on the relationship between the two discretized biweight density functions, truncated and nontruncated, jointly with the relationship between their respective truncated S_r^q and untruncated S_r discrete moments. The latter provide an approximation of the continuous moments μ_r , which improves as the asymmetric filter length increases. Similarly, the convergence of $S_r^q, q = 0, \dots, m$, to the

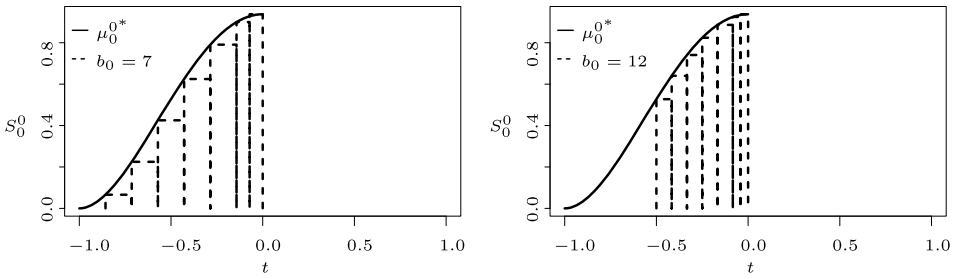


FIG. 4. Behavior of S_0^0 with $m = 6$, $b_0 = 7$ (left) and $b_0 = 12$ (right).

corresponding nontruncated moment S_r depends on the length of the asymmetric filter given by q and on the local bandwidth b_q . It should be noticed that b_q plays a very important role in the convergence property. For the last trend-cycle point weight, $q = 0$, (3.12) reduces to

$$w_{0,0} = \frac{\mu_4}{S_0^0 \mu_4 - S_2^0 \mu_2} \frac{15}{16b_0}.$$

It is apparent that the larger b_0 , the smaller is the weight given to the last trend-cycle point. Since the sum of all the weights of the last point asymmetric filter, $w_{0,-m}, \dots, w_{0,0}$, must be equal to one, this implies that the weights for the remaining points are very close to one another. This can be seen in Figure 4 (right side) that shows, for $m = 6$, the truncated continuous biweight density function and its discretized version when b_0 is equal to 12. The opposite is observed when b_0 is smaller, as shown in the same figure (left side) for b_0 equal to 7. Since a larger weight is given to the last point, much smaller weights have to be assigned to the remaining ones for all of them to add to one. Next, we introduce time-varying local bandwidths to improve the properties of the asymmetric filters in terms of size of revisions and time delay to signal the upcoming of true turning points.

4. Optimal bandwidth selection. The main effects induced by a linear filter on a given input are fully described in the frequency domain by its transfer function

$$\Gamma(\omega) = \sum_{j=-m}^m w_j \exp(-i2\pi\omega j), \quad \omega \in [-1/2, 1/2],$$

where, for better interpretation, the frequencies ω are given in cycles for unit of time instead of radians. Here, $\Gamma(\omega)$ represents the Fourier transform of the filter weights, $w_j, j = -m, \dots, m$, and it relates the spectral density $h_y(\omega)$ and $h_g(\omega)$ of the input and of the output, respectively, by

$$h_g(\omega) = \Gamma(\omega)h_y(\omega).$$

Thus, the transfer function $\Gamma(\omega)$ measures the effect of the filter on the total variance of the input at different frequencies. It is generally expressed in polar coordinates

$$(4.1) \quad \Gamma(\omega) = G(\omega) \exp(-i2\pi\phi(\omega)),$$

so that the impact of the filter on a (complex-valued) series $y_t = \exp(i2\pi\omega t)$, for $\omega \in [-1/2, 1/2]$, is

$$\begin{aligned} \hat{g}_t &= \Gamma(\omega) \exp(i2\pi\omega t) \\ &= G(\omega) \exp(-i2\pi\phi(\omega)) \exp(i2\pi\omega t) \\ &= G(\omega) \exp\{i2\pi[\omega t - \phi(\omega)]\}. \end{aligned}$$

$G(\omega) = |\Gamma(\omega)|$ is the gain of the filter, which measures the amplitude of the output for a sinusoidal input of unit amplitude, whereas $\phi(\omega)$ is the phase function, which shows the shift in phase of the output compared with the input. Hence, the transfer function plays a fundamental role to measure that part of the total revisions due to filter changes.

The measure of total revisions introduced by Musgrave (1964) is

$$(4.2) \quad E \left[\sum_{j=-m}^q w_{q,j} y_{t-j} - \sum_{j=-m}^m w_j y_{t-j} \right]^2, \quad q = 0, \dots, m - 1,$$

where, in our case, $w_{q,j}$ and w_j are given by (3.12) and (3.8), respectively. This criterion can be expressed in the frequency domain as follows:

$$\begin{aligned} & E \left[\sum_{j=-m}^q w_{q,j} e^{i2\pi\omega(t-j)} - \sum_{j=-m}^m w_j e^{i2\pi\omega(t-j)} \right]^2 \\ (4.3) \quad &= E[(\Gamma_q(\omega) - \Gamma(\omega))e^{i2\pi\omega t}]^2 \\ &= \int_{-1/2}^{1/2} |\Gamma_q(\omega) - \Gamma(\omega)|^2 e^{i4\pi\omega t} h_y(\omega) d\omega, \end{aligned}$$

where $h_y(\omega)$ is the unknown spectral density of y_t , whereas $\Gamma_q(\omega)$ and $\Gamma(\omega)$ are the transfer functions corresponding to the asymmetric and symmetric filters, respectively. Similarly to (4.2), expression (4.3) shows that, as new observations become available, revisions are due to two sources: (a) the new innovations entering the input series, and (b) changes in the asymmetric filters. In order to improve the current trend-cycle prediction based on the asymmetric Henderson filters, we study that part of the revisions due to asymmetric filter changes. Because the estimation of the real time trend-cycle is done concurrently, that is using all of the data up to and including the most recent value, knowledge of the speed of convergence of the last point trend-cycle filter to the central one gives valuable information on how often the real time trend estimate should be revised.

The quantity $|\Gamma_q(\omega) - \Gamma(\omega)|^2$ accounts for the revisions due to filter changes [Dagum (1982a, 1982b)], and it can be decomposed using the law of cosines as follows:

$$(4.4) \quad \begin{aligned} |\Gamma_q(\omega) - \Gamma(\omega)|^2 &= |G_q(\omega) - G(\omega)|^2 + 2G_q(\omega)G(\omega)[1 - \cos(\phi_q(\omega))] \\ &= |G_q(\omega) - G(\omega)|^2 + 4G_q(\omega)G(\omega) \sin\left(\phi_q\left(\frac{\omega}{2}\right)\right)^2, \end{aligned}$$

where the phase shift for the symmetric filter is equal to 0 or $\pm\pi$, and where $1 - \cos(\phi_q(\omega)) = 2 \sin(\phi_q(\omega/2))^2$. Based on (4.4), the mean square filter revision error can be expressed as follows:

$$(4.5) \quad \begin{aligned} 2 \int_0^{1/2} |\Gamma_q(\omega) - \Gamma(\omega)|^2 d\omega &= 2 \int_0^{1/2} |G_q(\omega) - G(\omega)|^2 d\omega \\ &\quad + 8 \int_0^{1/2} G_q(\omega)G(\omega) \sin\left(\phi_q\left(\frac{\omega}{2}\right)\right)^2 d\omega. \end{aligned}$$

The first component reflects the part of the total mean square filter error which is attributed to the amplitude function of the asymmetric filter. On the other hand, the second term measures the distinctive contribution of the phase shift. The term $G_q(\omega)G(\omega)$ is a scaling factor which accounts for the fact that the phase function is dimensionless, that is, it does not convey level information [Wildi (2008)].

As previously discussed, once the length of the filter is chosen, the properties of the asymmetric filters derived in RKHS are strongly affected by the choice of the time-varying local bandwidths $b_q, q = 0, \dots, m - 1$. Here, we propose several criteria for bandwidth selection based on (4.5), and analyze the properties of the corresponding optimal filters. We define as optimal a filter that minimizes both revisions and time delay to detect a true turning point. The LHS of (4.5) is a measure of total filter revision that provides the best compromise between the amplitude function of the asymmetric filter (gain) and its phase function (time displacement) [Dagum (1982a, 1982b), Dagum and Laniel (1987)]. Optimal asymmetric filters in this sense can be derived using local bandwidth parameters selected according to the following criterion:

$$(4.6) \quad b_{q,\Gamma} = \min_{b_q} \sqrt{2 \int_0^{1/2} |\Gamma_q(\omega) - \Gamma(\omega)|^2 d\omega}.$$

Based on the decomposition of the total filter revision error provided in (4.5), further bandwidth selection criteria can be defined by emphasizing more the gain or phase shift effects, and/or by attaching varying importance to the different frequency components, depending on whether they appear in the spectrum of the initial time series or not. In the context of smoothing a monthly input, the frequency domain $\Omega = \{0 \leq \omega \leq 0.50\}$ can be partitioned in two main intervals: (1) $\Omega_S = \{0 \leq \omega \leq 0.06\}$ associated with cycles of 16 months or longer attributed

TABLE 1
Optimal bandwidth values selected for each of the biweight asymmetric filters corresponding to the 9-, 13- and 23-term Henderson symmetric filters

<i>q</i>	0	1	2	3
$b_{q,\Gamma}$	6.47	5.21	4.90	4.92
$b_{q,G}$	8.00	5.67	4.87	4.90
$b_{q,\phi}$	4.01	4.45	5.97	6.93

<i>q</i>	0	1	2	3	4	5
$b_{q,\Gamma}$	9.54	7.88	7.07	6.88	6.87	6.94
$b_{q,G}$	11.78	9.24	7.34	6.85	6.84	6.95
$b_{q,\phi}$	6.01	6.01	7.12	8.44	9.46	10.39

<i>q</i>	0	1	2	3	4	5	6	7	8	9	10
$b_{q,\Gamma}$	17.32	15.35	13.53	12.47	12.05	11.86	11.77	11.77	11.82	11.91	11.98
$b_{q,G}$	21.18	18.40	16.07	13.89	12.44	11.90	11.72	11.73	11.83	11.92	11.98
$b_{q,\phi}$	11.01	11.01	11.01	11.01	11.41	13.85	15.13	16.21	17.21	18.15	19.05

to the signal (trend-cycle) of the series, and (2) $\bar{\Omega}_S = \{0.06 < \omega \leq 0.50\}$ corresponding to short cyclical fluctuations attributed to the noise.

We derive a class of optimal asymmetric filters based on bandwidth parameters $b_q, q = 0, \dots, m - 1$, selected as follows:

$$(4.7) \quad b_{q,G} = \min_{b_q} \sqrt{2 \int_0^{1/2} |G_q(\omega) - G(\omega)|^2 d\omega}$$

and

$$(4.8) \quad b_{q,\phi} = \min_{b_q} \sqrt{2 \int_{\Omega_S} G_q(\omega)G(\omega)[1 - \cos(\phi_q(\omega))] d\omega}.$$

It has to be noticed that the minimization of the phase error in (4.8) is very close to minimizing the average phase shift in month for the signal, that is,

$$(4.9) \quad b_{q,\phi} = \min_{b_q} \left[\frac{1}{0.06} \int_{\Omega_S} \frac{\phi(\omega)}{2\pi\omega} d\omega \right].$$

Table 1 illustrates the bandwidth parameters $b_{q,\Gamma}, b_{q,G}, b_{q,\phi}, q = 0, \dots, m - 1$, derived as minimizers of (4.6), (4.7) and (4.9), respectively, corresponding to the 9-, 13- and 23-term symmetric filters.

It can be noticed that, as q approaches m , the bandwidth parameters selected to optimize the criteria (4.6) and (4.7) get closer to $m + 1$, that is the global bandwidth considered for the symmetric Henderson filter. Hence, based on the relationships

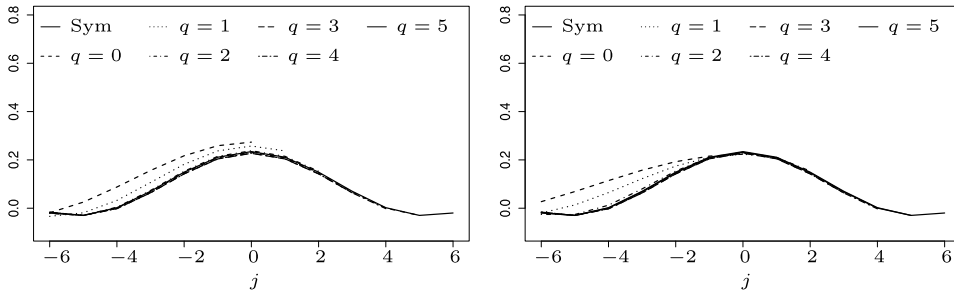


FIG. 5. Time path of the asymmetric filters based on $b_{q,\Gamma}$ (left), $b_{q,G}$ (right) corresponding to the 13-term symmetric filter.

between truncated and untruncated discrete biweight density functions and respective discrete moments previously discussed, the asymmetric filters based on $b_{q,\Gamma}$ and $b_{q,G}$, $q = 0, \dots, m - 1$, should be characterized by a fast convergence to the symmetric filter. This is confirmed by Figure 5 that illustrates, as an example, the time path of these filters corresponding to the 13-term symmetric one. Other filter lengths have been considered, but, for space reasons, we only show the results for the 13-term filter. However, similar conclusions can be drawn for different filter lengths.

The asymmetric filters based on $b_{q,\Gamma}$ and $b_{q,G}$, $q = 0, \dots, m - 1$, converge very fast to the symmetric filter, particularly after the previous to the last point, with the main differences observed for the last point filters. For these latter, the different behavior is analyzed in the frequency domain in Figure 6, that shows the corresponding gain and phase shift functions. It can be noticed that, as expected, the filter whose bandwidth $b_{0,G}$ is derived as minimizer of (4.7) shows a gain function closer to that of the symmetric Henderson filter than the one based on $b_{0,\Gamma}$, suppressing more noise at the highest frequencies, and it reproduces very well the signal in the lower frequency band.

In terms of phase shift or time delay, the filters that behave better are the ones based on the bandwidth parameters selected to minimize the average phase shift in months over the signal domain. However, as shown in Figure 7, their time path is

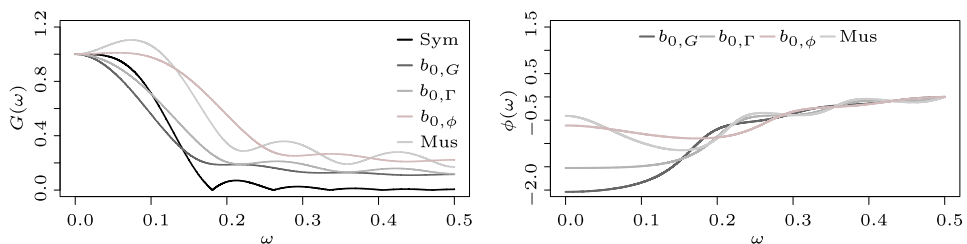


FIG. 6. Gain (left) and phase shift (right) functions for the last point asymmetric filters based on $b_{0,\Gamma}$, $b_{0,G}$ and $b_{0,\phi}$ compared with the last point Musgrave filter.

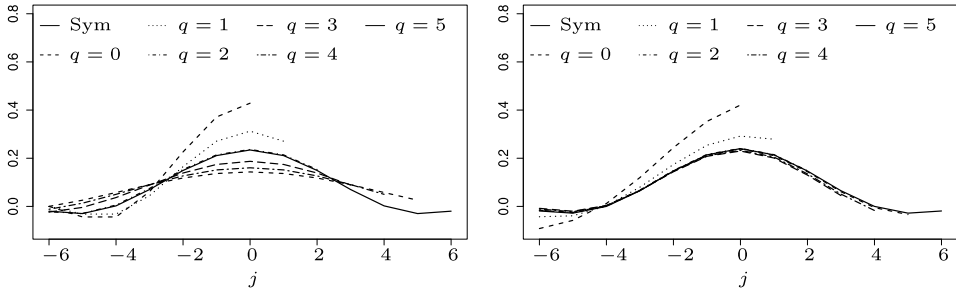


FIG. 7. Time path of the asymmetric filters based on $b_{q,\phi}$ (left) and of the Musgrave asymmetric filters (right) corresponding to the 13-term symmetric filter.

only very close to that of the filters derived by Musgrave (1964) up to $q = 2$, but there is no monotonic convergence of these asymmetric filters to their final one. This property is reflected in their phase shift function that, for the last point filter, is illustrated in Figure 6. As already said, the Musgrave filters are based on the minimization of the mean squared revision between the final estimates, obtained by the application of the symmetric filter, and the preliminary estimates, obtained by the application of an asymmetric filter, subject to the constraint that the sum of the weights is equal to one [Doherty (2001), Laniel (1985)]. These filters have the good property of fast detection of turning points.

As we can see, both the last point Musgrave filter and the one based on $b_{0,\phi}$ produce almost one half of the phase shift introduced by the filter based on $b_{0,\Gamma}$ and a quarter of the one introduced by the filter based on $b_{0,G}$ at the signal frequency band. However, the reduced phase shift produced by these two filters is compensated by larger revisions introduced in the final estimates. Indeed, as shown by the corresponding gain functions, the last point Musgrave filter and the one based on $b_{0,\phi}$ suppress much less noise than the filters obtained through minimization of (4.6) and (4.7). Furthermore, the Musgrave filter has the worst performance since it introduces a large amplification of the power attributed to the trend and suppresses less noise.

5. Application to the US economy. We have chosen a set of leading, coincident and lagging indicators of the US economy to illustrate some of the potential gains of using these new asymmetric filters. Time series that exhibit a turning point before the economy as a whole are called leading indicators, whereas those that change direction approximately at the same time are called coincident indicators. The lagging indicators are those that usually change direction after the whole economy does. The composite indexes are typically reported in financial and trade media. The series analyzed in this study are obtained from the St. Louis Federal Reserve Bank database, the Bureau of Labor Statistics, the Conference Board and the National Bureau of Economic Research (NBER). They are all final vintages

data in the sense that they will no longer be revised. We have chosen the following as leading indicators:

- Composite index of ten leading indicators (2010 = 100).¹
- Average weekly overtime hours, manufacturing.
- New orders for durable goods.
- New orders for nondefense capital goods.
- New private housing units authorized by building permits.
- Stock prices, S&P common stocks.
- Money supply, M2.
- Interest rate spread, 10-year treasury bonds less federal funds.
- Index of consumer expectation (University of Michigan).

We consider the following as coincident indicators:

- Composite index of four coincident indicators (2010 = 100).
- Employees on nonagricultural payrolls.
- Personal income less transfer payments.
- Industrial production index.
- Manufacturing and trade sales.

Finally, the lagging indicators treated are as follows:

- Composite index of seven lagging indicators (2010 = 100).
- Average duration of unemployment, weeks.
- Ratio, manufacturing and trade inventory to sale.
- Change in labor cost per unit of output, manufacturing.
- Commercial and industrial loans outstanding.

The asymmetric filters derived following the RKHS methodology versus the Musgrave filters, applied in conjunction with the symmetric Henderson filter, are evaluated as follows.

5.1. *Reduction of revision size in real time short-term trend estimates.* The reduction of revisions in real time trend-cycle estimates is very important because the estimates are preliminary and often used to assess the current stage of the economy. Statistical agencies and major users of these indicators are reluctant to large revisions because these can lead to wrong decision taking and policy making concerning the current economic situation. The series considered are all seasonally adjusted, where also trading day variations and extreme values have been removed if present. The indicators are series of different length, but the periods selected sufficiently cover the various lengths published for these series. For each series,

¹The index is rebased to average 100 in 2010. The history of the index is multiplied by 100 and divided by the average for the twelve months of the based year, currently 2010.

TABLE 2
Ratio of the mean square percentage revision errors of the last point asymmetric filters based on $b_{0,G}$, $b_{0,\Gamma}$ and $b_{0,\phi}$, and the last point Musgrave filter

Macro-area	Series	$\frac{b_{0,G}}{\text{Mus}}$	$\frac{b_{0,\Gamma}}{\text{Mus}}$	$\frac{b_{0,\phi}}{\text{Mus}}$
Leading	Composite index of ten leading indicators	0.503	0.643	0.933
	Average weekly overtime hours: Manufacturing	0.492	0.630	0.922
	New orders for durable goods	0.493	0.633	0.931
	New orders for nondefense capital goods	0.493	0.633	0.931
	New private housing units authorized by building permits	0.475	0.651	0.927
	S&P 500 stock price index	0.454	0.591	0.856
	M2 money stock	0.508	0.655	0.932
	10-year treasury constant maturity rate	0.446	0.582	0.849
	University of Michigan: Consumer sentiment	0.480	0.621	0.912
Coincident	Composite index of four coincident indicators	0.504	0.651	0.931
	All employees: total nonfarm	0.517	0.666	0.951
	Real personal income excluding current transfer receipts	0.484	0.627	0.903
	Industrial production index	0.477	0.616	0.884
	Manufacturing and trade sales	0.471	0.606	0.869
Lagging	Composite index of seven lagging indicators	0.523	0.653	0.966
	Average (mean) duration of unemployment	0.509	0.649	0.937
	Inventory to sales ratio	0.483	0.618	0.894
	Index of total labor cost per unit of output	0.515	0.663	0.983
	Commercial and industrial loans at all commercial banks	0.473	0.610	0.871

the length of the filters is selected according to the I/C (noise to signal) ratio, as classically done in the X11/X12ARIMA procedure [Ladiray and Quenneville (2001)]. In the sample, the ratio ranges from 0.20 to 1.98, hence filters of length 9 and 13 terms are applied.

The comparisons are based on the relative filter revisions between the final symmetric filter S and the last point asymmetric filter A , that is,

$$(5.1) \quad R_t = \frac{S_t - A_t}{S_t}, \quad t = 1, \dots, N.$$

For each series and for each estimator, we calculate the ratio between the Mean Square Percentage Error (MSPE) of the revisions corresponding to the filters derived following the RKHS methodology and those corresponding to the last point Musgrave filter. For all the estimators, the results illustrated in Table 2 show that the ratio is always smaller than one, indicating that the kernel last point predictors, based on time-varying bandwidth parameters, introduce smaller revisions than the Musgrave filter. This implies that the estimates obtained by the former will be more accurate than those derived by the application of the latter. In particular, as

expected, the best performance is shown by the filter based on the optimal bandwidth $b_{0,G}$ derived to minimize the criterion (4.7). In almost all the series its ratio with the last point Musgrave filter is less than one half and, on average, around 0.489. This implies that when applied to real data, the filter based on $b_{0,G}$ produces a reduction of almost fifty percent of the revisions introduced in the real time trend-cycle estimates given by the Musgrave filter. The filter based on $b_{0,\Gamma}$, derived to minimize the size of total filter revisions as defined by (4.6), also performs very well with more than thirty percent of revision reduction with respect to the Musgrave filter. In this case, the ratio is greater than the one corresponding to the filter based on $b_{0,G}$, but always less than 0.7 for all the series, being, on average, around 0.631. The filter whose bandwidth parameter is selected to minimize the average phase shift over the signal domain performs more similarly to the last point Musgrave filter but still shows revisions reduction, on average, around ten percent.

5.2. *Turning point detection.* It is important that the reduction of revisions in real time trend-cycle estimates is not achieved at the expense of increasing the time lag to detect the upcoming of a true turning point. A turning point is generally defined to occur at time t if (*downturn*)

$$y_{t-k} \leq \dots \leq y_{t-1} > y_t \geq y_{t+1} \geq \dots \geq y_{t+m}$$

or (*upturn*)

$$y_{t-k} \geq \dots \geq y_{t-1} < y_t \leq y_{t+1} \leq \dots \leq y_{t+m}.$$

Following Zellner, Hong and Min (1991), we have chosen $k = 3$ and $m = 1$ given the smoothness of the trend-cycle data. For each estimator, the time lag to detect the true turning point is affected by the convergence path of its asymmetric filters \mathbf{w}_q , $q = 0, \dots, m - 1$, to the symmetric one \mathbf{w} .

To determine the time lag needed by an indicator to detect a true turning point, we calculate the number of months it takes for the real time trend-cycle estimate to signal a turning point in the same position as in the final trend-cycle series. For the series analyzed in this paper, the time delays for each estimator are shown in Table 3. It can be noticed that the filters based on the bandwidth $b_{q,\phi}$ take two months (on average) as the Musgrave filters to detect the turning point. This is due to the fact that, even if $b_{q,\phi}$ filters are designed to be optimal in timeliness, their convergence path to the symmetric filter is slower and not monotone.

On the other hand, the filters based on $b_{q,\Gamma}$, $q = 0, \dots, m - 1$, and $b_{q,G}$, $q = 0, \dots, m - 1$, perform strongly better. In particular, whereas the former detect the turning point with an average time delay of 1.44 months, the latter takes 1.22 months.

The faster the upcoming of a turning point is detected, the faster new policies can be applied to counteract the impact of the business cycle stage. Failure to

TABLE 3
Time lag in detecting true turning points for the asymmetric filters based on $b_{q,G}$, $b_{q,\Gamma}$ and $b_{q,\phi}$, and the Musgrave filters

Series		$b_{q,G}$	$b_{q,\Gamma}$	$b_{q,\phi}$	Musgrave
Leading	Composite index of ten leading indicators	1	1	3	3
	Average weekly overtime hours: Manufacturing	1	1	1	1
	New orders for durable goods	1	2	3	2
	New orders for nondefense capital goods	1	2	2	3
	New private housing units authorized by building permits	2	2	3	3
	S&P 500 stock price index	1	2	2	2
	10-year treasury constant maturity rate	1	1	1	2
	University of Michigan: Consumer sentiment	1	1	1	1
Coincident	Composite index of four coincident indicators	1	1	2	2
	All employees: total nonfarm	1	1	1	2
	Real personal income excluding current transfer receipts	1	1	1	1
	Industrial production index	1	1	1	1
	Manufacturing and trade sales	1	2	3	3
Lagging	Composite index of seven lagging indicators	1	1	3	3
	Average (mean) duration of unemployment	3	3	4	3
	Inventory to sales ratio	1	1	1	2
	Index of total labor cost per unit of output	2	2	3	2
	Commercial and industrial loans at all commercial banks	1	1	1	1
Average time lag in months		1.22	1.44	2.00	2.06

recognize the downturn in the cycle or taking a long time delay to detect it may lead to the adoption of policies to curb expansion when, in fact, a recession is already underway.

To better highlight how the proposed filters perform when applied to series that are impacted differently by the short-term trend, we look at the revision path of the corresponding estimates. In this regard, we compare the performance of the filters on the three composite indicators, namely, leading, coincident and lagging, illustrated in Figure 8 for the period January 1995–December 2014. The composite index of ten leading indicators presents a deep turning point on May 2009, whereas shallow turning points are shown by the coincident and lagging composite indicators on August 2009 and May 2010, respectively.

Figure 9 exhibits the behavior of the Musgrave filters (right) and of the kernel filters based on $b_{q,G}$ in detecting the May 2009 turning point of the composite leading index. In particular, the figure shows the revision path of the last available point (May 2009) as we keep adding one observation at a time up to October 2009, when the final estimate is achieved.

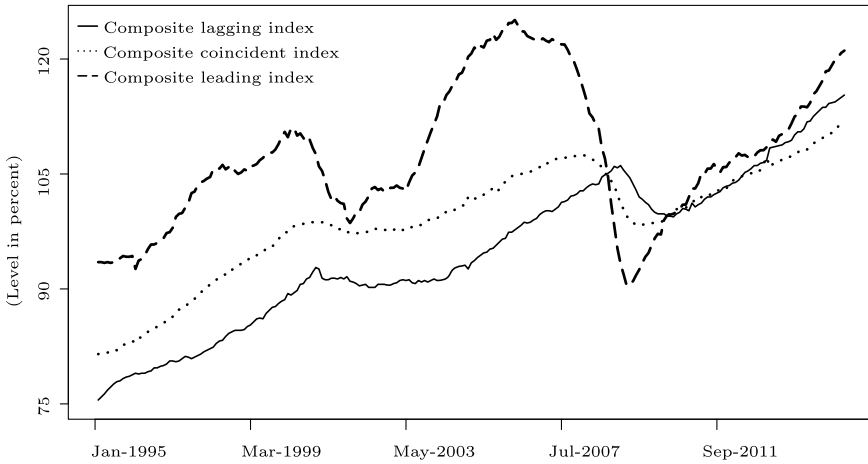


FIG. 8. Composite leading, coincident and lagging indicators of the US economy (2010 = 100).

It can be noticed that after adding one month at the series ending at May 2009, the turning point is clearly detected by the kernel filters, whereas three months are required by the Musgrave ones.

A similar pattern is observed in Figures 10 and 11 that are the “porcupine” graphs for the August 2009 and May 2010 turning points of the coincident and lagging composite indicators, respectively. For both series, the kernel filters detect the turning points after one month they have occurred, whereas the Musgrave filters take two months for the former, and three months for the latter. Hence, based on our previous considerations, the filters based on local bandwidth parameters selected to minimize criterion (4.7) are optimal, since they drastically reduce the total revisions by one half with respect to the Musgrave filters and, similarly, almost by one half the number of months needed to detect a true turning point.

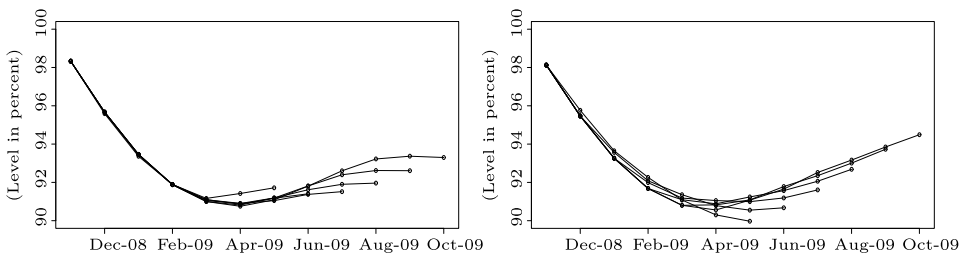


FIG. 9. Composite index of ten leading indicators (2010 = 100): revision path of the May 2009 (turning point) estimate as one observation is added at a time up to November 2009 (final estimate) using the asymmetric kernels based on $b_{q,G}$ (left) and Musgrave (right) filters, respectively.

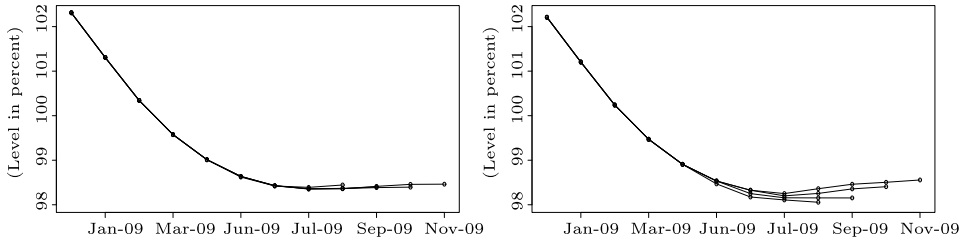


FIG. 10. Composite index of four coincident indicators (2010 = 100): revision path of the August 2009 (turning point) estimate as one observation is added at a time up to November 2009 (final estimate) using the asymmetric kernels based on $b_{q,G}$ (left) and Musgrave (right) filters, respectively.

6. Discussion. This paper deals with the problem of assessing, in real time, the direction of the short-term trend with an application to some key indicators of the US economy. The linear asymmetric filters here proposed are developed using the RKHS methodology. Given the length of the RKHS asymmetric filter, its properties strongly depend on the bandwidth parameter of the asymmetric kernel function from which the filter weights are derived. Since the m asymmetric filters corresponding to a $2m + 1$ symmetric filter are time varying, one for each specific point, we are here proposing local time-varying bandwidth parameters. We consider three main criteria for bandwidth selection in order to determine an optimal smoother. An optimal filter is defined as the one that minimizes revisions and time lag to detect the upcoming of a true turning point. The three main criteria of bandwidth parameter selection are minimization of the following: (1) the distance between the gain functions of asymmetric and symmetric filters, (2) the distance between the transfer functions of asymmetric and symmetric filters, and (3) the phase shift function over the domain of the signal.

We show theoretically that any of the three criteria produces asymmetric trend-cycle filters to be preferred to those developed by Musgrave concerning both size of revisions and time delay to detect the upcoming of true turning points. To highlight how the proposed filters perform when applied to series that are impacted

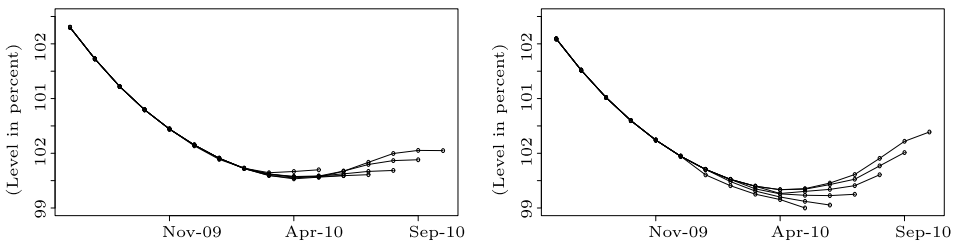


FIG. 11. Composite index of seven lagging indicators (2010 = 100): revision path of the May 2010 (turning point) estimate as one observation is added at a time up to November 2010 (final estimate) using the asymmetric kernels based on $b_{q,G}$ (left) and Musgrave (right) filters, respectively.

differently by the long-term trend, we look at the revision path of the corresponding estimates. In this regard, we compare the performance of the filters on three composite indicators, namely, leading, coincident and lagging. The composite index of ten leading indicators presents a deep turning point on May 2009, whereas shallow turning points are shown by the coincident and lagging composite indicators on August 2009 and May 2010, respectively. The real time trend-cycle filter calculated with the bandwidth parameter that minimizes the distance between the asymmetric and symmetric filters gain functions is to be preferred. This last point trend-cycle filter reduces around one half the size of the total revisions as well as the time delay to detect a true turning point with respect to the Musgrave filter. The new set of asymmetric kernel filters can be applied in many fields, such as economics, finance, health, hydrology, meteorology, criminology, physics, labor markets, utilities and so on, in fact, in any time series where the impact of trend plus cyclical variations is of relevance. For interested readers, the weight systems of these filters are given in the supplementary material [Dagum and Bianconcini (2015)] for 9- and 13-term symmetric filters.

APPENDIX: PROOF OF PROPOSITION 3.1

As shown by Dagum and Bianconcini [(2008) and (2013)], the symmetric filter weights are derived as follows:

$$w_j = \frac{K_4(j/b)}{\sum_{j=-m}^m K_4(j/b)}, \quad j = -m, \dots, m,$$

where b is the time-invariant global bandwidth parameter (same for all $t = m + 1, \dots, N - m$) selected to ensure a symmetric filter of length $2m + 1$. Based on (3.5), we obtain that

$$\begin{aligned} w_j &= \frac{\det(\mathbf{H}_4^0[1, \mathbf{j}/\mathbf{b}])(1/b) f_{0B}(j/b)}{\sum_{j=-m}^m \det(\mathbf{H}_4^0[1, \mathbf{j}/\mathbf{b}])(1/b) f_{0B}(j/b)} \\ &= \frac{\det(\mathbf{H}_4^0[1, \mathbf{j}/\mathbf{b}])(1/b) f_{0B}(j/b)}{\det(\mathbf{H}_4^0[1, \sum_{j=-m}^m \mathbf{j}/\mathbf{b}](1/b) f_{0B}(j/b))} \\ &= \frac{\det(\mathbf{H}_4^0[1, \mathbf{j}/\mathbf{b}])(1/b) f_{0B}(j/b)}{\det(\mathbf{H}_4^0[1, \mathbf{S}])} = \frac{\det(\mathbf{H}_4^0[1, \mathbf{j}/\mathbf{b}])(1/b) f_{0B}(j/b)}{\det(\mathbf{H}_s)}, \end{aligned}$$

where $\mathbf{H}_s = \mathbf{H}_4^0[1, \mathbf{S}]$, with $\mathbf{S} = [S_0^b, 0, S_2^b, 0]'$, and $S_r^b = 0$ for odd r . The expression above is exactly the same as we would obtain by solving for $\hat{\beta}_0 = \hat{g}_t$ the system of linear equations

$$\mathbf{H}_s \boldsymbol{\beta} = \mathbf{X}' \mathbf{F} \mathbf{y}.$$

Indeed, setting $\mathbf{c} = \mathbf{X}'_b \mathbf{F} \mathbf{b} \mathbf{y}$, the first coordinate of the solution vector is

$$\hat{\beta}_0 = \frac{\det(\tilde{\mathbf{H}}_4^0[1, \mathbf{c}])}{\det(\mathbf{H}_s)} = \frac{\det(\mathbf{H}_4^0[1, \mathbf{c}])}{\det(\mathbf{H}_s)}.$$

Given that $\mathbf{c} = \sum_{j=-m}^m (\mathbf{j}/\mathbf{b})(1/b) f_{0B}(j/b) y_{t+j}$, it follows that

$$\det(\mathbf{H}_4^0[1, \mathbf{b}]) = \sum_{j=-m}^m \det\left(\mathbf{H}_4^0\left[1, \frac{\mathbf{j}}{\mathbf{b}}\right]\right) \frac{1}{b} f_{0B}\left(\frac{j}{b}\right) y_{t+j}$$

and, therefore,

$$\hat{g}_t = \sum_{j=-m}^m \frac{\det(\mathbf{H}_4^0[1, \mathbf{j}/\mathbf{b}])(1/b) f_{0B}(j/b)}{\det(\mathbf{H}_s)} y_{t+j}.$$

Hence,

$$\hat{\beta}_0 = \mathbf{e}'_1 \mathbf{H}_s^{-1} \mathbf{X}'_b \mathbf{F}_b \mathbf{y},$$

and it follows that

$$\mathbf{w}' = \mathbf{e}'_1 \mathbf{H}_s^{-1} \mathbf{X}'_b \mathbf{F}_b.$$

Acknowledgments. We are indebted to the Editor Professor Brendan Murphy for his valuable comments that helped to enrich a previous version of this manuscript. We also want to thank the Associate Editor and two referees for their insightful suggestions and comments.

SUPPLEMENTARY MATERIAL

Weight systems (DOI: [10.1214/15-AOAS856SUPP](https://doi.org/10.1214/15-AOAS856SUPP); .pdf). The supplementary material contains the weight systems of our filters for 9- and 13-term symmetric filters.

REFERENCES

- AZEVEDO, J. V. (2011). A multivariate band-pass filter for economic time series. *J. R. Stat. Soc. Ser. C. Appl. Stat.* **60** 1–30. [MR2758567](#)
- AZEVEDO, J. V., KOOPMAN, S. J. and RUA, A. (2006). Tracking the business cycle of the Euro area: A multivariate model-based bandpass filter. *J. Bus. Econom. Statist.* **81** 575–593.
- BERLINET, A. (1993). Hierarchies of higher order kernels. *Probab. Theory Related Fields* **94** 489–504. [MR1201556](#)
- BERLINET, A. and THOMAS-AGNAN, C. (2004). *Reproducing Kernel Hilbert Spaces in Probability and Statistics*. Kluwer Academic, Boston, MA. [MR2239907](#)
- BIANCONCINI, S. and QUENNEVILLE, B. (2010). Real time analysis based on reproducing Kernel Henderson filters. *Estud. Econ. Aplicada.* **28** 553–574.
- CHOLETTE, P. A. (1981). Time series analysis. In *Proceedings of the Third International Conference (ITSM) Held in Houston, Tex., August 14–15, 1980* (O. D. Anderson and M. R. Perryman, eds.). North-Holland, Amsterdam. [MR0636789](#)
- CHRISTIANO, L. and FITZGERALD, T. (2003). The band-pass filter. *Internat. Econom. Rev.* **44** 435–465.
- DAGUM, E. B. (1982a). Revisions of time varying seasonal filters. *J. Forecast.* **1** 173–187.

- DAGUM, E. B. (1982b). The effects of asymmetric filters on seasonal factor revisions. *J. Amer. Statist. Assoc.* **77** 732–738.
- DAGUM, E. B. (1996). A new method to reduce unwanted ripples and revisions in trend-cycle estimates from X11ARIMA. *Wiley Ser. Surv. Methodol.* **22** 77–83.
- DAGUM, E. B. and BIANCONCINI, S. (2008). The Henderson smoother in reproducing kernel Hilbert space. *J. Bus. Econom. Statist.* **26** 536–545. [MR2459350](#)
- DAGUM, E. B. and BIANCONCINI, S. (2013). A unified view of nonparametric trend-cycle predictors via reproducing kernel Hilbert spaces. *Econometric Rev.* **32** 848–867. [MR3041105](#)
- DAGUM, E. B. and BIANCONCINI, S. (2015). Supplement to “A new set of asymmetric filters for tracking the short-term trend in real time.” DOI:10.1214/15-AOAS856SUPP.
- DAGUM, E. B. and LANIEL, N. (1987). Revisions of trend-cycle estimators of moving average seasonal adjustment methods. *J. Bus. Econom. Statist.* **5** 177–189.
- DAGUM, E. B. and LUATI, A. (2009a). A note on the statistical properties of nonparametric trend estimators by means of smoothing matrices. *J. Nonparametr. Stat.* **21** 193–205. [MR2488154](#)
- DAGUM, E. B. and LUATI, A. (2009b). A cascade linear filter to reduce revisions and false turning points for real time trend-cycle estimation. *Econometric Rev.* **28** 40–59. [MR2655618](#)
- DAGUM, E. B. and LUATI, A. (2012). Asymmetric filters for trend-cycle estimation. In *Economic Time Series* 213–230. CRC Press, Boca Raton, FL. [MR3076017](#)
- DE CARVALHO, M., RODRIGUES, P. C. and RUA, A. (2012). Tracking the US business cycle with a singular spectrum analysis. *Econom. Lett.* **114** 32–35.
- DE CARVALHO, M. and RUA, A. (2014). Nowcasting the US business cycle: Singular spectrum analysis at work. Working paper 16, Banco de Portugal.
- DOHERTY, M. (2001). The surrogate Henderson filters in X-11. *Aust. N. Z. J. Stat.* **43** 385–392. [MR1872198](#)
- FINDLEY, D. F. and MARTIN, D. E. K. (2006). Frequency domain analyses of SEATS and X-11/12-ARIMA seasonal adjustment filters for short and moderate-length time series. *J. Off. Stat.* **22** 1–34.
- GASSER, T. and MÜLLER, H.-G. (1979). Kernel estimation of regression functions. In *Smoothing Techniques for Curve Estimation (Proc. Workshop, Heidelberg, 1979). Lecture Notes in Math.* **757** 23–68. Springer, Berlin. [MR0564251](#)
- GRAY, A. and THOMSON, P. (1996). Design of moving-average trend filters using fidelity and smoothness criteria. In *Athens Conference on Applied Probability and Time Series Analysis, Vol. II* (1995) (P. M. Robinson and M. Rosenblatt, eds.). *Lecture Notes in Statist.* **115** 205–219. Springer, New York. [MR1466747](#)
- GRAY, A. G. and THOMSON, P. J. (2002). On a family of finite moving-average trend filters for the ends of series. *J. Forecast.* **21** 125–149.
- HENDERSON, R. (1916). Note on graduation by adjusted average. *Trans. Amer. Math. Soc.* **17** 43–48.
- HODRICK, R. J. and PRESCOTT, E. C. (1997). Postwar US business cycles: An empirical investigation. *J. Money Credit Bank.* **29** 1–16.
- KENNY, P. and DURBIN, J. (1982). Local trend estimation and seasonal adjustment of. *Economic and Social Time Series. J. Roy. Stat. Soc. A Stat.* **145** 1–41.
- KYUNG-JOON, C. and SCHUCANY, W. R. (1998). Nonparametric kernel regression estimation near endpoints. *J. Statist. Plann. Inference* **66** 289–304. [MR1614481](#)
- LADIRAY, D. and QUENNEVILLE, B. (2001). *Seasonal Adjustment with the X-11 Method*. Springer, New York.
- LANIEL, N. (1985). Design criteria for the 13-term Henderson end weights. Working paper, Methodology Branch, Statistics Canada. Ottawa.
- LOADER, C. (1999). *Local Regression and Likelihood*. Springer, New York. [MR1704236](#)
- MUSGRAVE, J. (1964). A set of end weights to end all end weights. Working paper, US Census Bureau, Washington, DC.

- QUENNEVILLE, B., LADIRAY, D. and LEFRANCOIS, B. (2003). A note on musgrave asymmetrical trend-cycle filters. *J. Forecast.* **19** 727–734.
- SHISKIN, J., YOUNG, A. and MUSGRAVE, J. (1967). The X-11 Variant of the Census Method II Seasonal Adjustment Program. Technical paper 15.
- WILDI, M. (2008). *Real-Time Signal Extraction: Beyond Maximum Likelihood Principles*. Springer, Berlin.
- ZELLNER, A., HONG, C. and MIN, C. (1991). Forecasting turning points in international output growth rates using Bayesian exponentially weighted autoregression, time-varying parameter, and pooling techniques. *J. Econometrics* **49** 275–304.

DEPARTMENT OF STATISTICAL SCIENCES
UNIVERSITY OF BOLOGNA
VIA BELLE ARTI, 41 - 40126 BOLOGNA
ITALY
E-MAIL: estela.beedagum@unibo.it